Defence Technology 17 (2021) 1617–1624

Contents lists available at ScienceDirect

Defence Technology

journal homepage: www.keaipublishing.com/en/journals/defence-technology

Influence of propagation direction on operation performance of rotating detonation combustor with turbine guide vane

Wan-li Wei, Yu-wen Wu*, Chun-sheng Weng, Quan Zheng

National Key Laboratory of Transient Physics, Nanjing University of Science and Technology, Nanjing, 210094, China

ARTICLE INFO

Article history:
Received 23 June 2020
Received in revised form
27 July 2020
Accepted 25 August 2020
Available online 28 August 2020

Keywords:
Rotating detonation combustor
Propagation direction
Turbine guide vane
Operation performance

ABSTRACT

Due to the pressure gain combustion characteristics, the rotating detonation combustor (RDC) can enhance thermodynamic cycle efficiency. Therefore, the performance of gas-turbine engine can be further improved with this combustion technology. In the present study, the RDC operation performance with a turbine guide vane (TGV) is experimentally investigated. Hydrogen and air are used as propellants while hydrogen and air mass flow rate are about 16.1 g/s and 500 g/s and the equivalence ratio is about 1.0. A pre-detonator is used to ignite the mixture. High-frequency dynamic pressure transducers and silicon pressure sensors are employed to measure pressure oscillations and static pressure in the combustion chamber. The experimental results show that the steady propagation of rotating detonation wave (RDW) is observed in the combustion chamber and the mean propagation velocity is above 1650 m/s, reaching over 84% of theoretical Chapman-Jouguet detonation velocity. Clockwise and counterclockwise propagation directions of RDW are obtained. For clockwise propagation direction, the static pressure is about 15% higher in the combustor compared with counterclockwise propagation direction, but the RDW dominant frequency is lower. When the oblique shock wave propagates across the TGV, the pressure oscillations reduces significantly. In addition, as the detonation products flow through the TGV, the static pressure drops up to 32% and 43% for clockwise and counterclockwise propagation process respectively.

1. Introduction

Detonation is a supersonic combustion in which a shock wave is propagated driven by an energy release in the reaction zone [1]. Compared with deflagration, detonation owns low entropy increase and faster heat release rate. Rotating detonation combustion chamber is a new machine which makes detonation wave continuously propagate in annular combustor to generate thrust. The rotating detonation combustor (RDC) has many advantages, such as high thermal efficiency, fast heat release rate, simple and compact structure [2,3]. In recent years, RDC has been examined as a possible alternative method to improve the performance of the propulsion system. Most of the research on RDC focuses on the ignition and initiation process, detonation wave propagation mode and stability. Fotia et al. [4] identified the impact of different geometric and flow parameters on the ignition processes in a laboratory scale RDC. Bluemner et al. [5] investigated on the rotating detonation wave (RDW) mode transition dynamics in a hydrogen-air RDC, they found that mass flow rate and equivalence ratio coupled with the plenum pressures were the driving parameters for RDW mode transition. Anand et al. [6,7] conducted a detailed study on the instability of detonation wave propagation process and compared this instability with the rocket engine [8].

Due to the pressure gain of detonation wave and the high thermodynamic cycle efficiency [9], it is feasible to replace the constant pressure combustor of aero-turbine engine with RDC. The rotating detonation aero-turbine engine (RDATE) can improve the combustion efficiency, reduce the number of compressors and simplify the structure of the engine. In recent years, scholars have carried out relevant research. Frolov et al. [10] verified the feasibility of integrating the RDC and a gas turbine engine via three-dimensional numerical simulation. The results showed the RDC exhibited a gain in the total pressure of 15% as compared with the same combustion chamber operating in the deflagration mode. Meanwhile, they also proposed that the pressure disturbance propagating upstream from RDC towards compressor could be

* Corresponding author.
E-mail address: y.wu@njust.edu.cn (Y.-w. Wu).
Peer review under responsibility of China Ordnance Society

https://doi.org/10.1016/j.dt.2020.08.009

almost completely suppressed by designing a suitable upstream isolator. In addition, they found the inclination angle of turbine guide vane (TGV) and the direction of RDW could change the operation mode of RDC [11]. The pressure fluctuation was obviously suppressed by the TGV, but the temperature was hardly affected. Sousa et al. [12] proposed a numerical tool to calculate and analyze the thermodynamic process and non-isentropic process of RDATE. By comparing the combustion efficiency of RDATE with the conventional constant pressure combustor, they found that the efficiency of RDATE is at least 5% higher at the low pressure ratio. Ji et al. [13] put forward a complete scheme of a dual-duct RDATE and analyzed its overall performance. Compared with the constant pressure combustor under the same parameters, they found that RDATE had a greater advantage in performance and there existed an optimum pressure ratio that maximizes the thermal efficiency.

Scholars not only carried out relevant research in theoretical analysis but also explored in experiments. Wolanski et al. [14] studied the stability of rotating detonation wave and selected the optimal structure of RDC to replace the conventional constant pressure combustor of GTD-350 turboshaft engine. The experimental results showed that the performance of RDATE was 7% higher than the original engine. Ishiyama et al. [15] and Higashi et al. [16]. Successfully obtained the RDW on a disc RDC with single-stage centrifugal compressor and single-stage radial turbine. They analyzed several combustion modes and observed the number of detonation waves, quenching and re-ignition phenomena by streak pictures. Naples et al. [17,18] used the RDC and constant pressure combustor to drive T63 gas turbine respectively. They found that RDC had higher unsteadiness than traditional constant pressure combustor, but the higher unsteadiness had little impact on turbine efficiency. Zhou et al. [19,20] combined RDC and an axial-flow turbine to investigate the propagation characteristics of RDW. They found that the high frequency pressure oscillations decreased after the TGV and the TGV had a certain impact on the detonation wave propagation speed and stability. Welsh et al. [21] designed an integration assembly for attaching the nozzle guide vane to RDC. Pressure, temperature, and unsteadiness measurements were completed to characterize the exhaust flow of the RDE through the TGV. They found that stagnation pressure dropped an average of 5% through the TGV. Bach et al. [22] developed a configurable, instrumented guide vane for characterizing the performance of RDC. They found that the pressure rise through the combustor increased significantly with increasing mass flow rate.

Past research on RDATE focused on the feasibility verification and the performance analysis. The mechanism of the interaction between RDW and TGV is still unclear, especially when RDW propagates in different direction. According to the relative position of the RDW and the TGV, the propagation process of the RDW can be divided as clockwise and counterclockwise direction, as shown in Fig. 1. The expansion process of detonation products and the reflection of the oblique shock wave at the TGV are different for the two propagation directions. It is necessary to know the influence of propagation direction on operation performance to make the RDATE practical application successfully. In the present study, experiments were carried out with hydrogen as fuel and air as oxidant on an RDC integration with a TGV. The operation process of the two propagation directions, the influence of propagation direction on the characteristics of RDW, the high-frequency pressure oscillations, and the static pressure upstream and downstream of TGV were analyzed in detail. This study may provide some theoretical and engineering bases for enriching the research of RDATE.

2. Experimental system and measurement method

As shown in Fig. 2, the experimental system consists of an RDC, a TGV with aerodynamic vanes, a propellants delivery system, and a control and signal acquisition system.

The propellants delivery system provides fuel and oxidizer for the RDC and the pre-detonation tube. Hydrogen and air flow through the pressure reducing valve, sonic nozzle, flowmeter, solenoid valve and check valve in turn. The propellant mass flow rate and equivalence ratio can be adjusted by reducing valve and the supply time of propellant can be controlled by solenoid valve. The mass flow rate is measured by E + H mass flowmeter and the maximum error of mass flowmeter is ±0.35%. Fig. 3 is the physical drawing of the RDC and TGV. The inner diameter, outer diameter and the length of the RDC are 78 mm, 88 mm and 130 mm, respectively. The chord length of the TGV is 25.5 mm, the blade height is 21 mm, the number of blades is 13, and the angle between axis and chord line is 52°. Air is injected into the RDC through an annular slit and the size of the annular throat is 1.2 mm. Hydrogen is injected into the RDC through 60 orifices whose diameter is 0.8 mm evenly distributed over the inner wall. In order to guarantee the propagation direction of RDW unchanged during the entire observation time, the mass air flow rate is 500 ± 2 g/s, the hydrogen mass flow rate is 16.1 g/s, the equivalence ratio is about 1.0, and the operation condition is the same for all tests. The ambient temperature and pressure are 293 K and 1 atm respectively.

Four PCB transducers are arranged on the outside wall of the RDC to measure the pressure signals of RDW. Another two PCB transducers (113b26) are installed at upstream and downstream of the TGV to acquire the pressure oscillations. The positions of the PCB pressure transducers are shown in Fig. 4. The measured signal is recorded by the NI data acquisition system. Five diffusion silicon pressure sensors (Omega PX409) with the accuracy of ±0.08% BSL

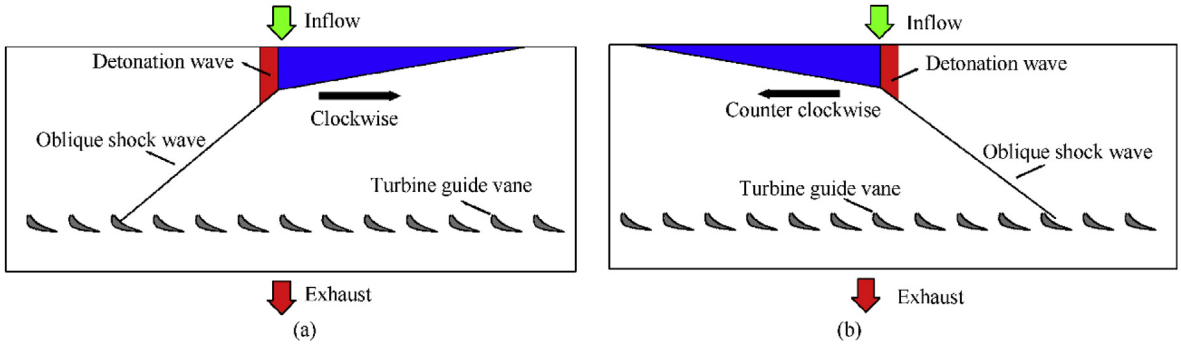

Fig. 1. Schematic diagram of propagation direction: (a) clockwise; (b) counterclockwise.

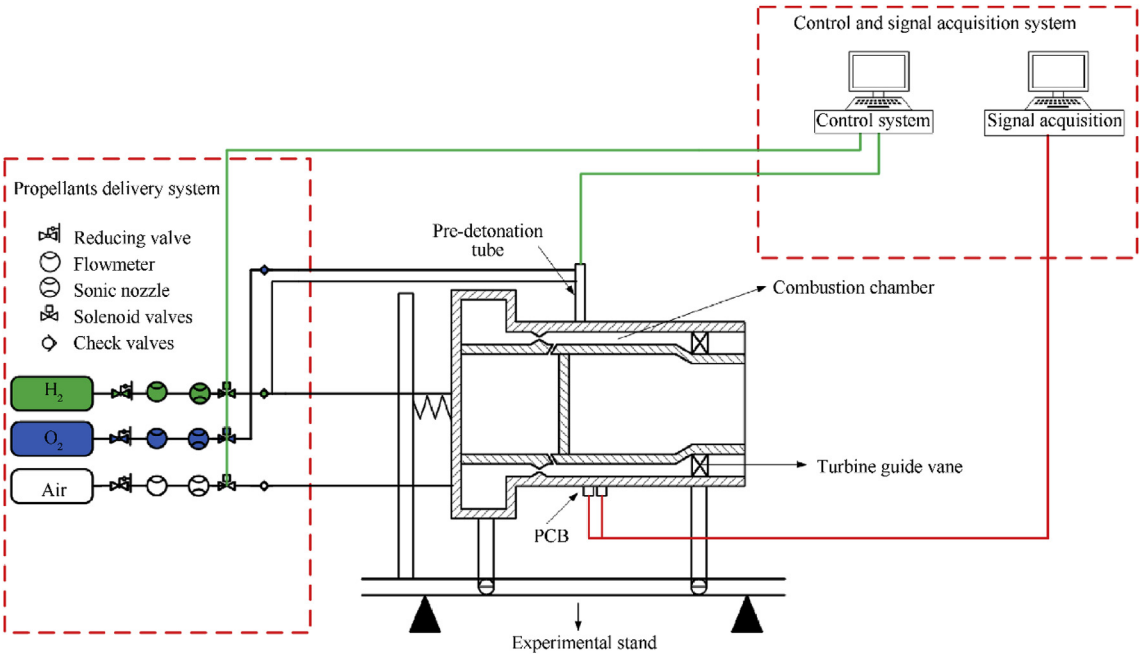

Fig. 2. Schematic diagram of the experiment system.

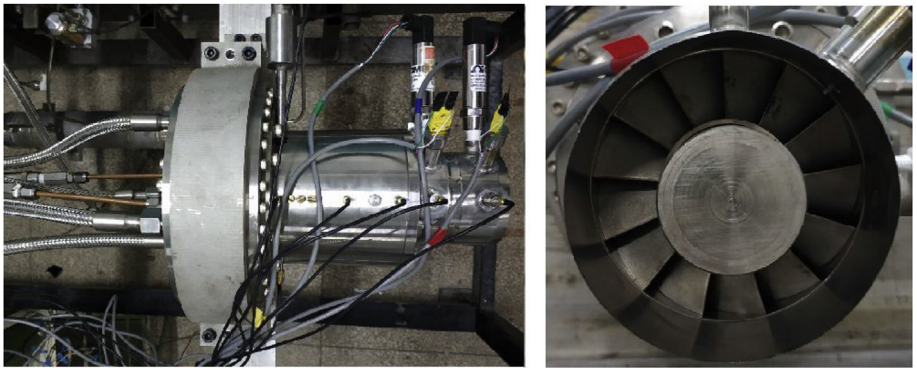

Fig. 3. Physical drawing of RDC and TGV.

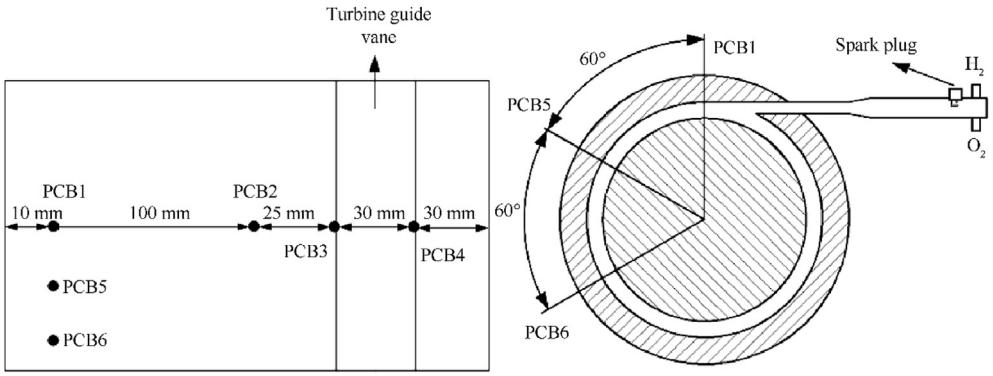

Fig. 4. Locations of sensors.

are installed to measure the static pressure in the hydrogen plenum (S_h), air plenum (S_a), combustor (S_c), upstream (S_u)and downstream (S_d) of the turbine guide, respectively. The experimental time sequence is shown in Fig. 5. A control and data acquisition system is used to control the time sequence and records experimental signals. More details related to the RDC configuration and control system are described in Ref. [23].

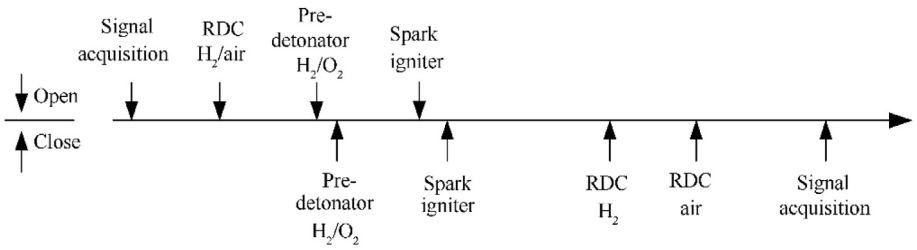

Fig. 5. Experimental time sequence.

3. Analysis of propagation process

A typical test for RDW clockwise propagation process is shown in Fig. 6, where t_1, t_2 and t_3 represent are the start, ignition and end time of propellant. The pressure in the hydrogen and air plenum rises rapidly and reaches equilibrium in a short time at t_1, and the pressure in the combustor increases slightly as well. To remain the air and hydrogen mass flow rate relatively stable, the propellants delivery system operates 1000 ms prior to the ignition. The RDC is successfully initiated at t_2 and S_c rises to 3.13 bar rapidly. S_a and S_h rise to 7.58 bar and 8.36 bar due to the pressure rise in the combustor. The RDC operates from 0 ms to 420 ms and stops operating at t_3, which is enough to form the stable propagation of RDW. As shown in Fig. 6(b), when the initial detonation enters from the pre-detonation tube to the annular combustor, it takes a short period of time t_{DDT} to form the RDW. The RDW sequentially passes P6 and P5, indicating a clockwise propagation from the end view.

As shown in Fig. 6(c), it can be clearly observed the variation of the dominant frequency during the whole operation process of RDW initiation, stable propagation and quenching. The propagation frequency of RDW rapidly reaches about 5990 Hz after ignition and the dominant frequency of RDW remains steady during the operation of RDC. In the quenching phase of RDW, the dominant frequency of RDW rapidly decreases.

Fig. 7 shows a typical RDW counterclockwise propagation process test. Fig. 7(a) shows the pressure histories of combustor and plenums during the operation. S_a, S_h and S_c are in accord with clockwise test from t_1 to t_2. At t_2, S_a, S_h and S_c rise to a relatively stable value of 8.34 bar, 7.61 bar and 2.69 bar, respectively. Compared with the clockwise propagation case, only S_c is decreased. Fig. 7(b) shows the similar phenomena of low pressure oscillations prior to the RDW initiation. However, the self-sustained RDW passes through P5 and P6 sequentially, indicating a counterclockwise propagation of RDW from the end view. It is clearly seen from Fig. 7(c) that the domain frequency of RDW stabilizes at 6100 Hz and terminates at 340 ms. It is found that the S_c of counterclockwise propagation process is lower than that of clockwise propagation process. The propagation direction of RDW will affect the pressure of combustor S_c apparently. Subsequently, the influence of propagation direction on RDW propagation characteristics will be discussed in the next section.

4. Influence on RDW propagation characteristics

Fig. 8(a) and (b) show the magnified pressure-time distributions of PCB5 and PCB6 for the clockwise and counterclockwise propagation tests. The peak pressures of RDW range from 12 bar to 23 bar. The results obtained via Fast Fourier Transformation (FFT) analysis for PCB6 are shown in Fig. 8(c) and (d). The dominant frequencies f_{dom} of clockwise and counterclockwise test are 5991 Hz and 6073 Hz respectively. The RDW propagation velocity is calculated by $v_{ave} = \pi D_0 f_{dom}$, where D_0 is the combustor outer diameter. The average velocities of clockwise and counterclockwise test are 1655.4 m/s and 1678.1 m/s respectively. The theoretical CJ velocity calculated by NASA CEA code [24] is 1964.6 m/s. The velocity deficits are about 15.74% and 14.58% of clockwise and counterclockwise test respectively.

The characteristics of S_c and f_{dom} are evaluated by repeated experiments. For all tests, only single-wave propagation mode is observed in the RDC. As shown in Fig. 9(a), for clockwise propagation tests, the pressure of combustor S_c is greater than counterclockwise propagation tests, rising about 15%. The main reason may lie in the presence of TGV at downstream of the RDC. The TGV is an asymmetric structure and detonation products do not flow along the axial direction, the flow condition of detonation products is different for clockwise and counterclockwise propagation process at the TGV. The flow deflection angle and flow resistance are smaller for counterclockwise propagation process, resulting in the decrease of combustor pressure S_c.

Fig. 9(b) shows that f_{dom} of counterclockwise propagation tests are above 6050 Hz, while f_{dom} of clockwise propagation tests are below 6000 Hz. For the same the operation condition, when the combustor pressure S_c increases, the injection ratio (combustor inlet total pressure divided by S_c) will decline. As stated by Schwer and Kailasanath [25], the propagation velocity of RDW was related to the RDW height, while the RDW height was determined by the injection ratio. The decrease of the injection ratio will lead to the reduction of RDW height, resulting in the detonation velocity deficits. This might be the reason of lower propagation frequency f_{dom} for clockwise propagation tests.

5. Influence on the pressure of the turbine guide vane

Two PCB transducers are installed at upstream and downstream of the TGV to acquire the dynamic pressure oscillations. Fig. 10 shows the pressure oscillations at upstream and downstream of the TGV. P3 is at upstream of the TGV and P4 is at downstream of the TGV. The signals of P3 show obvious different pressure oscillation phenomena for clockwise and counterclockwise propagation tests. The oblique shock wave is reflected at the TGV to form several reflection shock waves with smaller pressure peaks. The pressure peaks of reflection shock waves (blue dots) are about one third of oblique shock wave (red dots). Compared with the clockwise propagation tests, the reflection shocks of counterclockwise tests are more chaotic and complex. In addition, the TGV can significantly attenuate pressure oscillations and the pressure peaks reduce for both propagation directions throughout the operation.

Two diffusion silicon pressure sensors are installed at upstream and downstream of the TGV to acquire the static pressure distributions. Fig. 11 shows the data of static pressure at upstream and downstream of the TGV. $S_{u\_clockwise}$ and $S_{d\_clockwise}$ represent the static pressure at upstream and downstream of the TGV for clockwise propagation tests, while $S_{u\_counterclockwise}$ and $S_{d\_counterclockwise}$ represent the static pressure for counterclockwise propagation

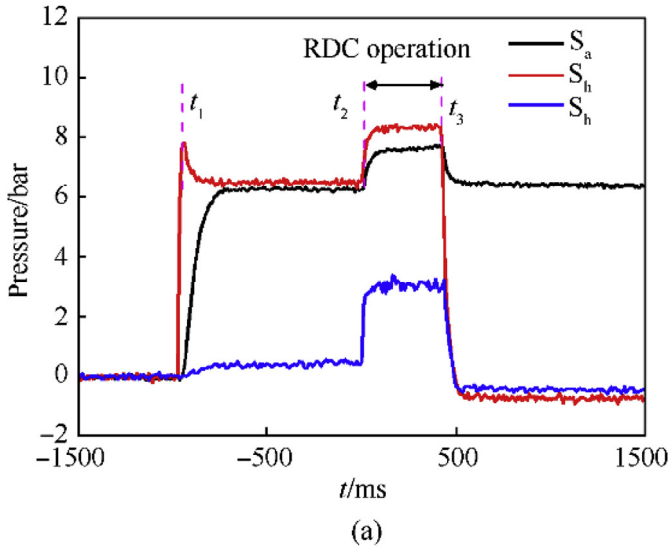

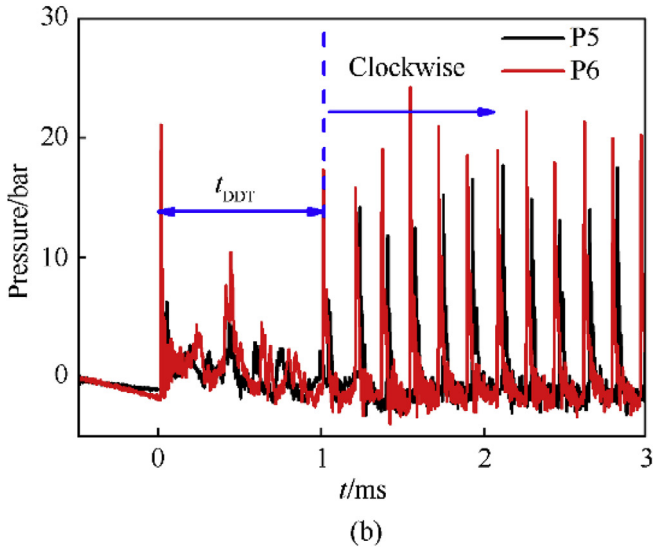

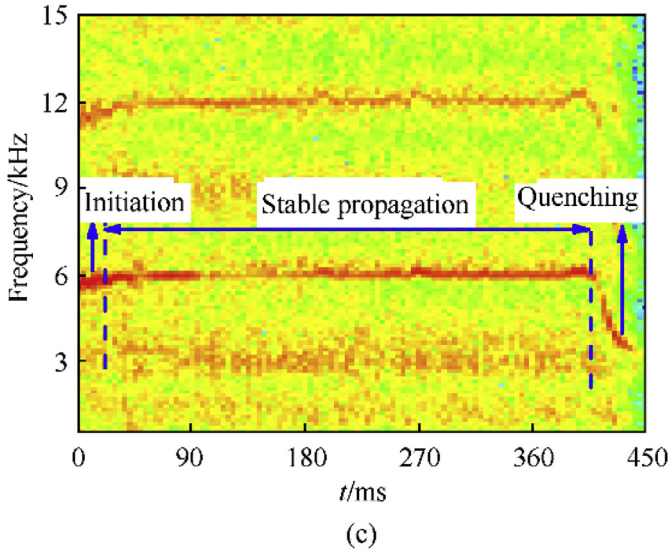

Fig. 6. Experimental results of clockwise test: (a) The pressure histories of combustor and plenums; (b) Initial stage of the PCB pressure curve; (c) Short Time Fourier Transform (STFT).

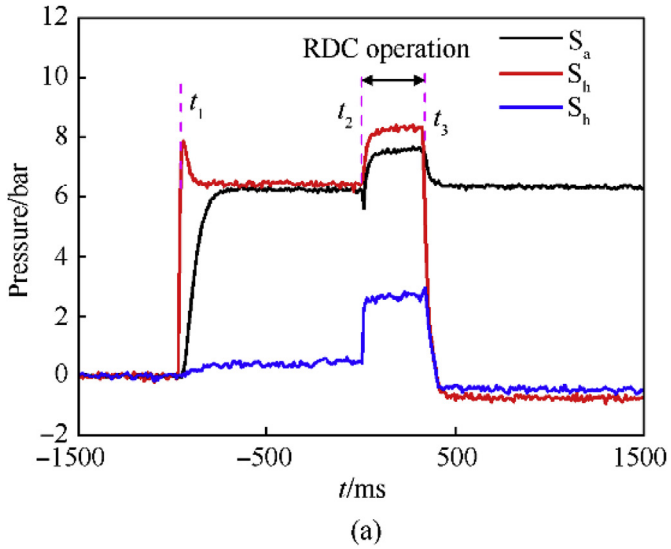

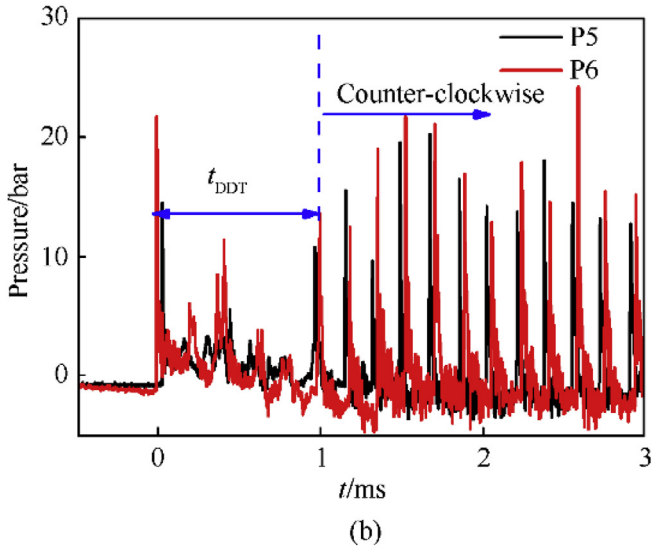

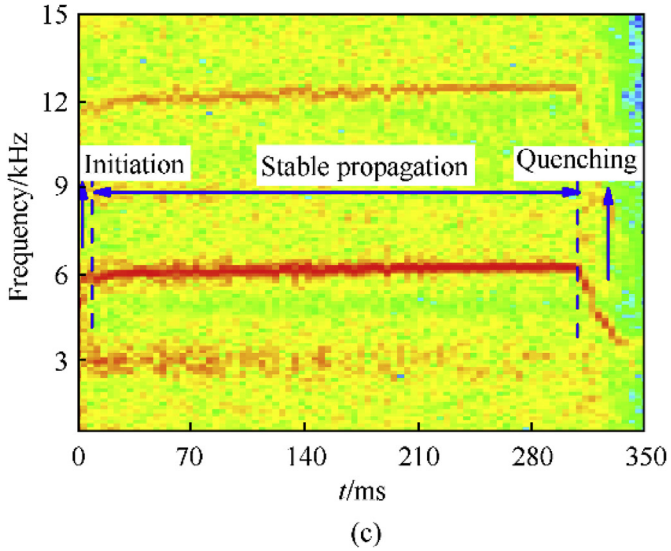

Fig. 7. Experimental results of counterclockwise tests: (a) The pressure histories of combustor and plenums; (b) Initial stage of the PCB pressure curve; (c)STFT.

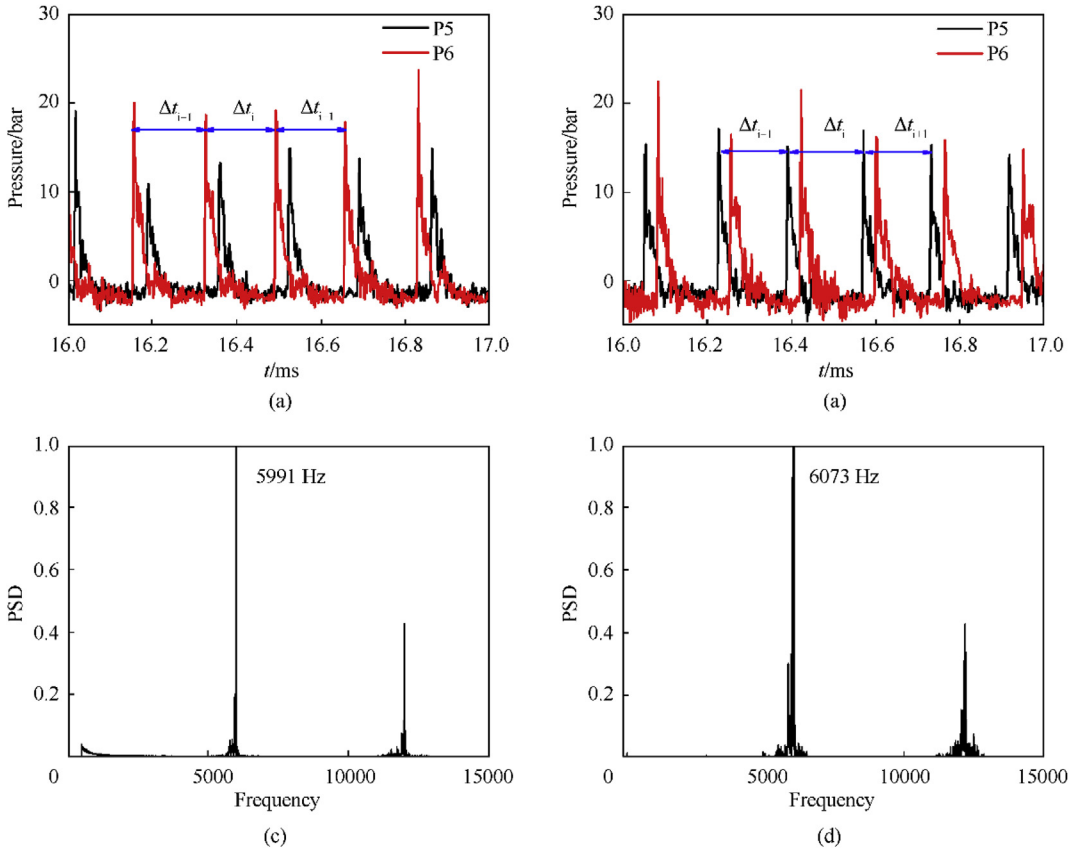

Fig. 8. Experimental results: (a) P5 and P6 for clockwise test; (b) P5 and P6 for counterclockwise test; (c) FFT results of P6 for clockwise tests; (d) FFT results of P6 for counterclockwise tests.

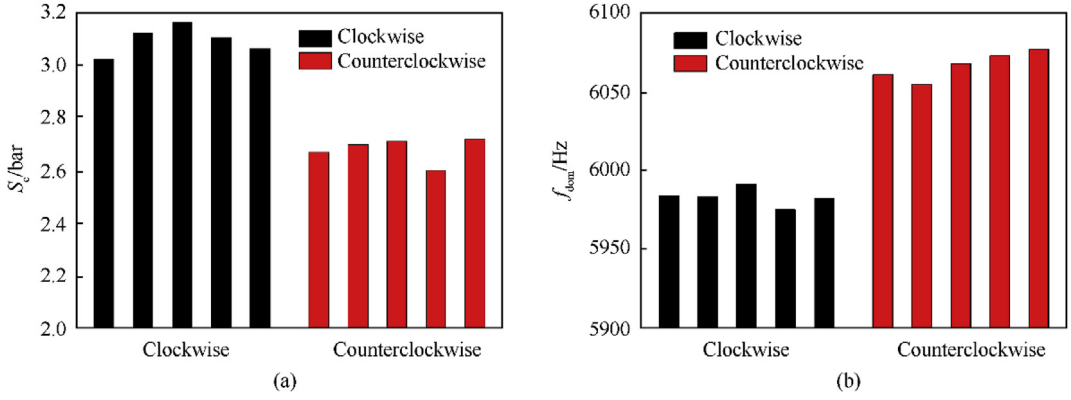

Fig. 9. The statistical results of repeated experiments: (a) The pressure of combustor; (b) The dominant frequency.

tests. It can be seen that the static pressure at downstream of the TGV is lower than that at upstream of the TGV for the both propagation directions, the static pressure is significantly reduced when the detonation products pass through the TGV. In addition, the values of $S_{u\_clockwise}$ and $S_{u\_counterclockwise}$ are about 0.68 bar of clockwise propagation tests and 0.63 bar of counterclockwise propagation tests. However, the propagation direction has great influence on the static pressure at downstream of the TGV, the static pressure at the downstream is about 0.46 bar of clockwise propagation tests and 0.36 bar of counterclockwise propagation tests, reducing by 32% and 43% respectively. Due to the angle between the oblique shock wave and the TGV, the number of reflected shock waves during clockwise propagation process is more than counterclockwise propagation process, multiple reflected shock waves increase the flow resistance of the TGV. This may be the main reasons for the static pressure drop is distinct for both propagation process. When the RDW propagates in counterclockwise for the TGV given in this paper, the flow resistance is small, the frequency is high, and the pressure drop is large. The counterclockwise propagation is more beneficial to improve the performance of the RDATE.

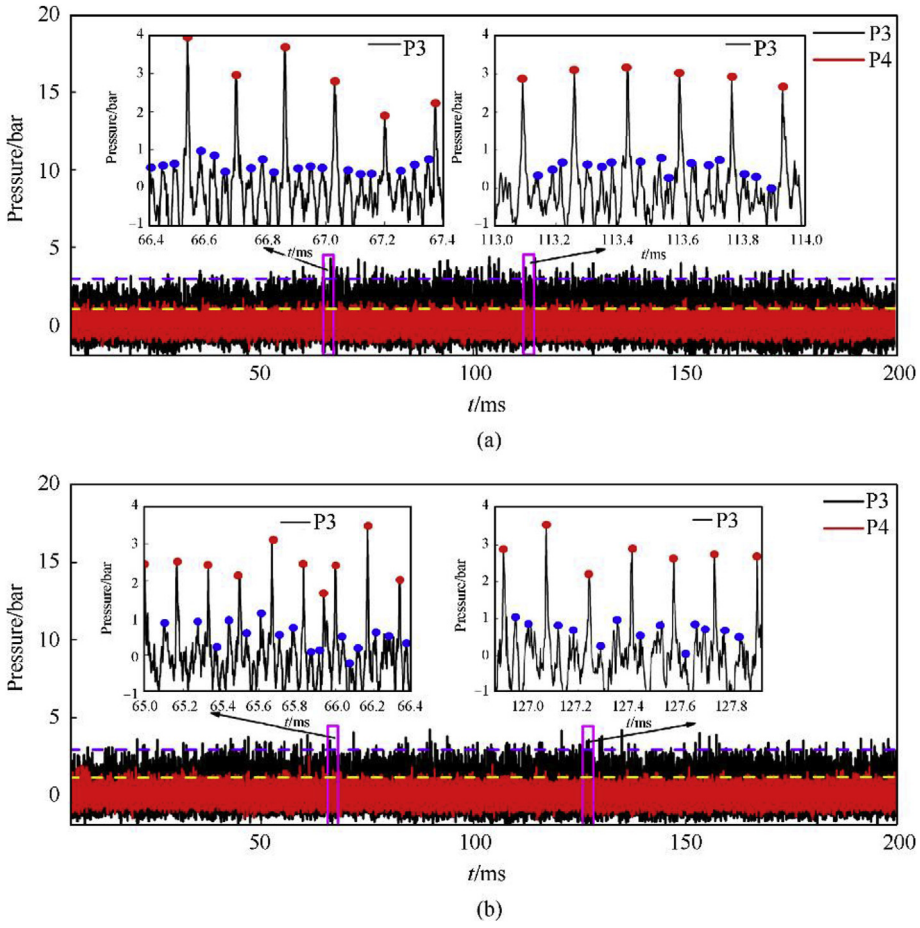

Fig. 10. The pressure oscillation at upstream and downstream of the TGV: (a) clockwise propagation; (b) counterclockwise propagation.

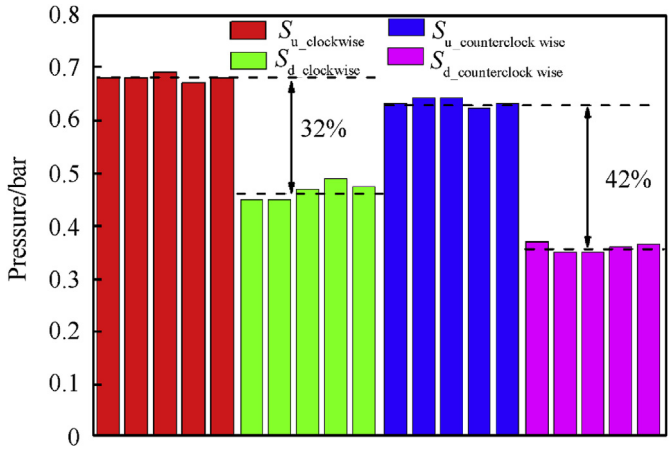

Fig. 11. The data of static pressure at TGV.

6. Conclusions

A hydrogen-air rotating detonation combustor model integrated with a turbine guide vane has been established. Experiments have been carried out to investigate its operation performance. For the given engine model operating under the condition of mass air flow rate of 500 g/s and equivalence ratio of about 1.0, the conclusions are drawn as follows:

(1) When the detonation wave formed in the pre-detonator enters into the RDC, the RDW cannot be initiated directly and it is formed after a complex, transitory period. Subsequently, the self-sustained propagating RDW is formed and two RDW states are obtained, namely, clockwise and counterclockwise propagation state. Also, only steady single-wave propagation mode is observed with repeated experiments. From STFT analysis, it clearly shows the RDW initiation, stable propagation and quenching process. The RDW propagation velocity is acquired about 1650 m/s, and the velocity deviation from the theoretical CJ value is less than 16%.

(2) When the RDW is initiated in the RDC, the static pressure in the combustion chamber grows remarkably. Comparing the data in the combustion chamber for clockwise and counterclockwise propagation tests, the static pressure is about 15% higher for clockwise propagation state. Meanwhile, the RDW propagation frequency show that the dominant frequency for counterclockwise propagation state is higher, reaching above 6050 Hz. The average velocity of RDW is higher when RDW propagates in counterclockwise.

(3) When the oblique shock wave propagates downstream to the TGV, the pressure oscillations can be significantly attenuated by the TGV. The oblique shock wave will be reflected at the TGV, the reflection shocks of counterclockwise propagation state are more chaotic and complex compared with the clockwise propagation state. In addition, the multiple reflected shock waves increase the flow resistance of the TGV. The static pressure at the downstream is about 0.46 bar for

clockwise propagation state and 0.36 bar of counterclockwise propagation state, reducing by 32% and 43% respectively.

Declaration of competing interest

The authors declare that they have no conflict of interest.

Acknowledgment

This work was supported by the National Natural Science Foundation of China (No. 11702143 and 11802137) and the Fundamental Research Funds for the Central Universities (No. 30918011343 and 30919011259).

References

[1] Lee JHS. The detonation phenomenon. NewYork: Cambridge University Press; 2008.
[2] Wolanski P. Detonative propulsion. Proc Combust Inst 2013;34:125–58.
[3] Rankin BA, Fotia ML, Naples AG, Stevens CA, Hoke JL, Kaemming TA, Theuerkauf SW, Schauer FR. Overview of performance, application, and analysis of rotating detonation engine technologies. J Propul Power 2017;33:131–43.
[4] Fotia ML, Hoke J, Schauer F. Study of the ignition process in a laboratory scale rotating detonation engine. Exp Therm Fluid Sci 2018;94:345–54.
[5] Bluemner R, Bohon MD, Paschereit CO, Gutmark EJ. Counter-rotating wave mode transition dynamics in an RDC. Int J Hydrogen Energy 2019;44:7628–41.
[6] Anand V, St George A, Driscoll R, Gutmark E. Characterization of instabilities in a rotating detonation combustor. Int J Hydrogen Energ 2015;40:16649–59.
[7] Anand V, St George A, Gutmark E. Amplitude modulated instability in reactants plenum of a rotating detonation combustor. Int J Hydrogen Energ 2017;42:12629–44.
[8] Anand V, Gutmark E. Rotating detonation combustors and their similarities to rocket instabilities. Prog Energy Combust Sci 2019;73:182–234.
[9] Frolov SM, Aksenov VS, Ivanov VS. Experimental proof of Zel'dovich cycle efficiency gain over cycle with constant pressure combustion for hydrogen-oxygen fuel mixture. Int J Hydrogen Energy 8 June 2015;40(Issue 21):6970–5.
[10] Frolov SM, Dubrovskii AV, Ivanov VS. Three-dimensional numerical simulation of a continuously rotating detonation in the annular combustion chamber with a wide gap and separate delivery of fuel and oxidizer//Progress in propulsion physics. In: Calabro M, DeLuca L, Frolov S, Galfetti L, Haidn O, editors. EUCASS advances in aerospace sciences book series, vol. 8. Moscow-Paris: TORUS PRESS - EDP Sciences; 2016. p. 375–88.
[11] Frolov SM, Dubrovskii AV, Ivanov VS. Three-dimensional numerical simulation of continuously rotating detonation inan annular combustor with an immovable turbine guide vane. Combust Explos 2014;7:136–43.
[12] Sousa J, Paniagua G, Collado Morata E. Thermodynamic analysis of a gas turbine engine with a rotating detonation combustor. Appl Energy 2017;195:247–56.
[13] Ji Z, Zhang H, Wang B. Performance analysis of dual-duct rotating detonation aero-turbine engine. Aero Sci Technol 2019;92:806–19.
[14] Wolanski P. Application of the continuous rotating detonation to gas turbine. Appl Mech Mater 2015;782:3–12.
[15] Ishiyama C, Miyazaki K, Nakagami S, Matsuoka K, Kasahara J, Matsuo A, Funaki I. Experimental study of research of centrifugal-compressor-radial-turbine type rotating detonation engine. Salt Lake City, UT, United states: American Institute of Aeronautics and Astronautics Inc, AIAA; 2016.
[16] Higashi J, Nakagami S, Matsuoka K, Kasahara J, Matsuo A, Funaki I, Moriai H. Experimental study of the disk-shaped rotating detonation turbine engine. In: 55th AIAA aerospace sciences meeting. Texas: Grapevine; 2017.
[17] Naples A, Hoke J, Battelle R, Schauer F. T63 turbine response to rotating detonation combustor exhaust flow. J Eng Gas Turbines Power 2019;141.
[18] Naples A, Hoke J, Battelle R, Wagner M, Schauer F. Rotating detonation engine implementation into an open-loop T63 gas turbine engine. Grapevine, TX, United states: American Institute of Aeronautics and Astronautics Inc.; 2017.
[19] Zhou S, Ma H, Li S, Liu D, Yan Y, Zhou C. Effects of a turbine guide vane on hydrogen-air rotating detonation wave propagation characteristics. Int J Hydrogen Energy 2017;42:20297–305.
[20] Zhou S, Ma H, Ma Y, Zhou C, Liu D, Li S. Experimental study on a rotating detonation combustor with an axial-flow turbine. Acta Astronaut 2018;151:7–14.
[21] Welsh DJ, King PI, Debarmore ND, Schauer FR, Hoke JL. RDE integration with T63 turboshaft engine components. In: American institute of aeronautics and astronautics inc., national harbor, MD, United States. AIRBUS; BOEING; DUNMORE; LOCKHEED MARTIN; 2014.
[22] Bach E, Bohon MD, Paschereit CO, Stathopoulos P. Development of an instrumented guide vane set for rdc exhaust flow characterization. Cincinnati, OH, United states: American Institute of Aeronautics and Astronautics Inc, AIAA; 2018.
[23] Li B, Wu Y, Weng C, Zheng Q, Wei W. Influence of equivalence ratio on the propagation characteristics of rotating detonation wave. Exp Therm Fluid Sci 2018;93:366–78.
[24] McBride BJ. Computer program for calculation of complex chemical equilibrium compositions and applications. NASA Lewis Research Center; 1996.
[25] Schwer D, Kailasanath K. Numerical investigation of the physics of rotating-detonation-engines. Proc Combust Inst 2011;33:2195–202.